



<b>Publication Year</b>	2024
<b>Acceptance in OA</b>	2025-02-04T16:12:18Z
<b>Title</b>	Snapshot of a magnetohydrodynamic disk wind traced with water masers
<b>Authors</b>	MOSCADELLI, Luca, SANNA, ALBERTO, Beuther, Henrik, Oliva, André, Kuiper, Rolf
<b>Publisher's version (DOI)</b>	10.1017/S1743921323002132
<b>Handle</b>	<a href="http://hdl.handle.net/20.500.12386/35804">http://hdl.handle.net/20.500.12386/35804</a>
<b>Serie</b>	PROCEEDINGS OF THE INTERNATIONAL ASTRONOMICAL UNION
<b>Volume</b>	vol. 18, S380

# Snapshot of a magnetohydrodynamic disk wind traced with water masers

Luca Moscadelli<sup>1</sup> , Alberto Sanna<sup>2,3</sup> , Henrik Beuther<sup>4</sup>,  
André Oliva<sup>5,6</sup>  and Rolf Kuiper<sup>7</sup> 

<sup>1</sup>INAF-Osservatorio Astrofisico di Arcetri, Largo E. Fermi 5, Firenze 50125, Italy.  
email: [luca.moscadelli@inaf.it](mailto:luca.moscadelli@inaf.it)

<sup>2</sup>INAF-Osservatorio Astronomico di Cagliari, Via della Scienza 5, Selargius (CA) 09047, Italy

<sup>3</sup>Max-Planck-Institut für Radioastronomie, Auf dem Hügel 69, Bonn 53121, Germany

<sup>4</sup>Max Planck Institute for Astronomy, Königstuhl 17, Heidelberg 69117, Germany

<sup>5</sup>Institut für Astronomie und Astrophysik, Auf der Morgenstelle 10, Tübingen 72076, Germany

<sup>6</sup>Space Research Center (CINESPA), Ciudad Universitaria Rodrigo Facio, San José 11501, Costa Rica

<sup>7</sup>Faculty of Physics, University of Duisburg-Essen, Lotharstraße 1, Duisburg 47057, Germany

**Abstract.** Disk-jet systems are common in astrophysical sources of different nature, from black holes to gaseous giant planets. The disk drives the mass accretion onto a central compact object and the jet ejects material along the disk rotation axis. Magnetohydrodynamic disk winds can provide the link between mass accretion and ejection, which is essential to ensure that the excess angular momentum is removed and accretion can proceed. However, up to now, we have been lacking direct observational proof of disk winds. This work presents a direct view of the velocity field of a disk wind around a forming massive star. Achieving a very high spatial resolution of 0.05 au, our water maser observations trace the velocities of individual streamlines emerging from the disk orbiting the forming star. We find that, at low elevation above the disk midplane, the flow co-rotates with its launch point in the disk, in agreement with magneto-centrifugal acceleration. Beyond the co-rotation point, the flow rises spiraling around the disk rotation axis along a helical magnetic field. We have performed (resistive-radiative-gravito-) magnetohydrodynamic simulations of the formation of a massive star and record the development of a magneto-centrifugally launched jet presenting many properties in agreement with our observations.

**Keywords.** ISM: jets and outflows, ISM: kinematics and dynamics, Stars: formation, Masers

---

## 1. Introduction

Accretion and ejection of matter are intimately related in different astrophysical objects covering a wide spectrum of masses, from black holes to gaseous giant planets. Magnetohydrodynamic (MHD) disk winds (Blandford and Payne 1982; Pudritz and Norman, 1983) can provide the link between mass accretion and ejection, but, so far, a direct observational proof of their existence has been lacking. The “Protostellar Outflows at the Earliest Stages” (POETS) survey (Moscadelli et al. 2016; Sanna et al. 2018) has recently imaged the disk/outflow interface on scales of 10–100 au in a statistically significant sample (37) of luminous YSOs, employing multi-frequency Jansky Very Large Array (JVLA) observations to determine the spatial structure of the ionized

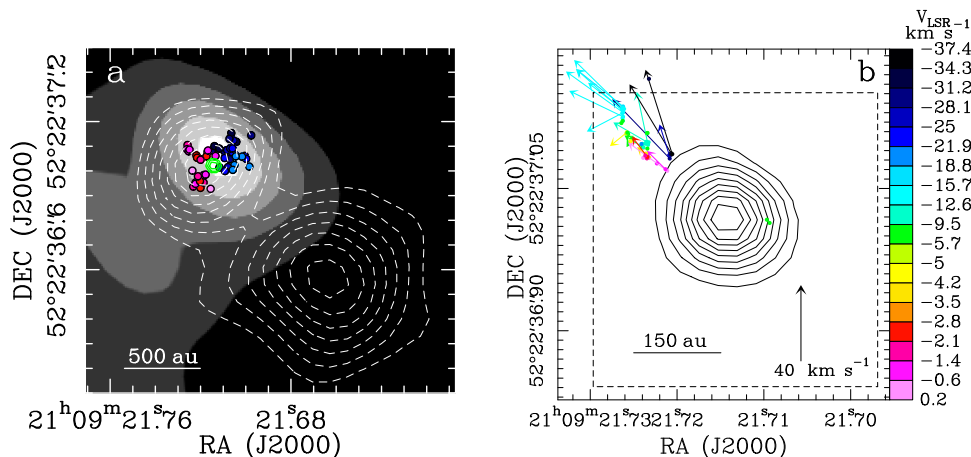


**Figure 1.** Previous NOEMA, JVLA and VLBA observations towards IRAS 21078+5211. (a) The gray-scale (from 10 to 35 mJy beam<sup>-1</sup>) map reproduces the NOEMA 1.37 mm continuum emission (Moscadelli *et al.* 2021). The colored dots represent the channel emission peaks of the CH<sub>3</sub>CN  $J_K = 12_K - 11_K$  ( $K = 3 - 6$ ) and HC<sub>3</sub>N  $J = 24 - 23$  lines, with colors denoting the channel  $V_{\text{LSR}}$ : blue for  $[-13.6, -10]$  and red  $[-2.5, 0.5]$  km s<sup>-1</sup>. The green (70%, 80%, and 90% of 0.50 mJy beam<sup>-1</sup>) and white (from 30% to 90%, in steps of 10% of 0.096 mJy beam<sup>-1</sup>) contours show the JVLA A-Array continuum at 1.3 cm and 5 cm, respectively. (b) Colored dots and arrows give absolute positions and proper motions of the 22 GHz water masers determined with multi-epoch (2010–2011) VLBA observations (Moscadelli *et al.* 2016), with colors denoting the maser  $V_{\text{LSR}}$ . The black contours (from 10% to 90%, in steps of 10% of 0.50 mJy beam<sup>-1</sup>) indicate the JVLA A-Array continuum at 1.3 cm. The dashed rectangle delimits the field of view plotted in Fig. 2a.

emission, and multi-epoch Very Long Baseline Array (VLBA) observations to derive the three-dimensional (3D) velocity distribution of the 22 GHz water masers. One of the most interesting POETS targets is the YSO IRAS 21078+5211 ( $L_{\text{bol}} \sim 5 \cdot 10^3 L_{\odot}$  at a distance of  $1.63 \pm 0.05$  kpc,  $M_{\text{YSO}} = 5.6 \pm 2 M_{\odot}$ ; Moscadelli *et al.* 2021). On scales of  $\sim 1000$  au (see Fig. 1a), the location of the YSO is marked by the peaks of the Northern Extended Millimeter Array (NOEMA) 1.3 mm, and JVLA 1.3 and 5 cm continuum emissions, well aligned in position within the observational errors. The 5 cm continuum presents two slightly resolved components oriented along SW-NE, and traces the radio jet powering the collimated molecular outflow revealed with the NOEMA SO emission at larger scales. The NOEMA CH<sub>3</sub>CN and HC<sub>3</sub>N channel emission centroids are red- and blue-shifted to SE and NW of the YSO, respectively, and their velocity pattern is best interpreted in terms of rotation, most likely within an accretion disk. The 22 GHz water masers emerge at separations between 100 and 200 au from the YSO (see Fig. 1b), pinpointed by the 1.3 cm continuum peak. The maser spatial distribution and proper motions are collimated along the jet/outflow direction, clearly indicating that the water masers are tracing the base of the radio jet. The analysis of the 3D maser motions, specifically the local standard of rest (LSR) velocity ( $V_{\text{LSR}}$ ) gradient transversal to the jet axis and the constant ratio between the toroidal and poloidal velocities, first suggested that the jet could be launched from a MHD disk wind.

## 2. Results

In October 2020, we have re-observed the water maser emission in IRAS 21078+5211 with global Very Long Baseline Interferometry (VLBI) observations achieving a sensitivity of 0.7 mJy beam<sup>-1</sup>, which has allowed us to detect weaker masers and sample a

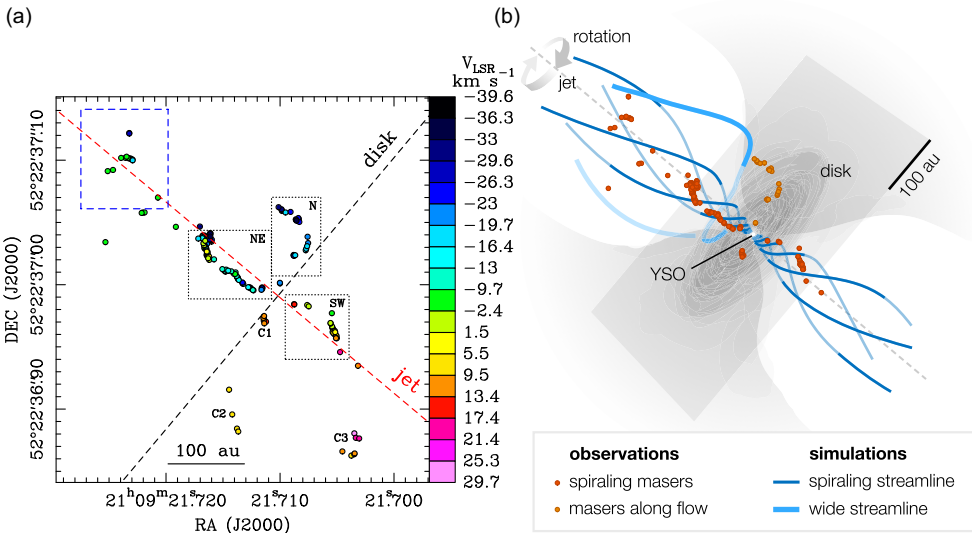


**Figure 2.** Global VLBI observations of the 22 GHz water masers and 3D view of the proposed kinematical interpretation (Moscadelli et al. 2022). (a) Colored dots give absolute positions of the 22 GHz water masers, with colors denoting the maser  $V_{LSR}$ . The black dotted rectangles encompass the three regions, to the N, NE and SW, where maser emission concentrate. The blue dashed rectangle delimits the area of maser emission in the previous VLBA observations. The red and black dashed lines mark the sky-projected jet and disk axis, respectively. (b) Observed maser positions (red and orange dots) overlaid on top of streamlines (blue curves) computed from resistive-radiative-gravito-MHD simulations of a jet around a forming massive star. The streamlines close to the rotation axis show significant spiraling motion, in agreement with the kinematic signature of the masers observed in the NE and SW regions. The wide streamline from the simulation illustrates the outflowing trajectory of material from the outer disk, similar to the observed masers in the N region. For context, the protostar, the disk and the outflow cavity have been sketched in gray, based on the density structure obtained in the simulations.

region closer to the YSO (Moscadelli et al. 2022). The maser emission concentrates in three regions to NE, N, and SW, inside the three dotted rectangles of Fig.2a. The jet (the dashed red line in Fig.2a) and disk (dashed black line) axes provide a convenient coordinate system to refer the maser positions to. The interpretation of the maser kinematics is based on the analysis of the three independent observables:  $z$ , the elevation above the disk plane (or offset along the jet),  $R$ , the radial distance from the jet axis (or transversal offset), and the maser  $V_{LSR}$ . The accuracy of the maser positions is  $\approx 0.05$  au, and that of the maser  $V_{LSR} \approx 0.5$  km s<sup>-1</sup>. We can express the maser velocities as the sum of two terms, one associated with the toroidal component or rotation around the jet axis,  $V_{rot}$ , and the other associated with the poloidal component including all the contributions owing to non-rotation,  $V_{off}$ . Since, as indicated by previous observations (Moscadelli et al. 2021), the jet axis is close to the plane of the sky and we observe the rotation close to edge-on, we can write:

$$V_{LSR} = V_{off} + V_{rot} = V_{off} + \omega \Sigma \sin(\phi) \tag{1}$$

$$R = \Sigma \sin(\phi) \tag{2}$$

where  $\phi$  is the angle between the rotation radius  $\Sigma$  and the line of sight, and  $\omega$  is the angular velocity.

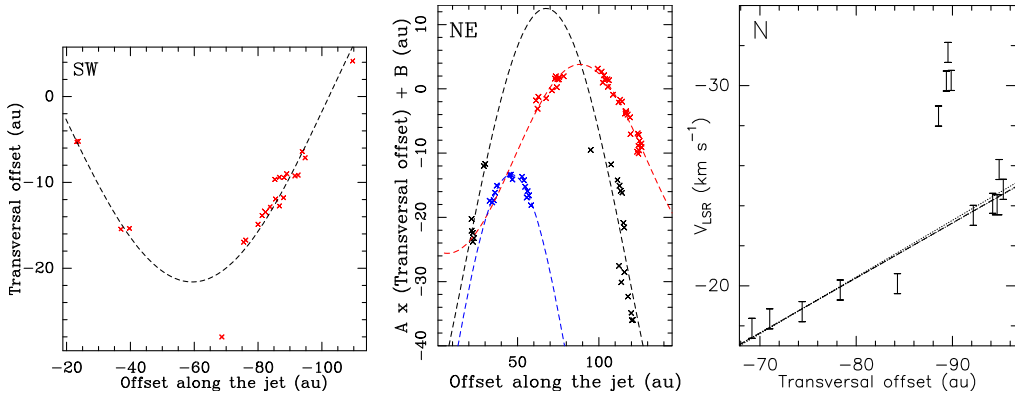


**Figure 3. The SW and NE spiral motions, and the magneto-centrifugally accelerated N stream.** (SW) Plot of the coordinates  $R$  versus  $z$  for the water masers in the SW region. The positional error is smaller than the cross size. The black dashed curve is the fitted sinusoid. (NE) Plot of the linear transformation of  $R$  versus  $z$  for the water masers in the NE region. Black, red, and blue colors refer to masers belonging to the NE-1, NE-2, and NE-3 streams, respectively. We plot the linear transformation of the radii to reduce the overlap and improve the visibility of each of the three streams. The dashed curves are the fitted sinusoids. (N) Plot of maser  $V_{\text{LSR}}$  versus  $R$  in the N region. Errorbars denote the maser  $V_{\text{LSR}}$  and corresponding  $2\sigma$  errors, and the black dashed and dotted lines show the best linear fit and the associated uncertainty, respectively. The linear fit of  $V_{\text{LSR}}$  versus  $R$  has been performed considering only the masers with  $V_{\text{LSR}} \geq -27 \text{ km s}^{-1}$ .

Figs. 3 SW and 3NE show the remarkable finding that the spatial coordinates  $z$  and  $R$  of the maser emission in both the SW and NE regions satisfy the relation:

$$R = C \sin(f_z(z - z_0)) \quad (3)$$

where  $C$ , the amplitude of the sinusoid,  $f_z$ , the spatial frequency, and  $z_0$ , the position of zero phase, are fitted constants. While in the SW region the water masers draw a single sinusoid, in the NE region they belong to three different sinusoidal streams (labeled NE-1, NE-2 and NE-3). The comparison of Eqs. 2 and 3 leads to a straightforward interpretation of the sinusoidal relation between the coordinates by taking: 1)  $\Sigma = C$ , and 2)  $\phi = f_z \|z - z_0\|$ . The former equation indicates that the rotation radius is the same for all the masers, the latter shows that the motions of rotation around and streaming along the jet axis are locked together, which is the condition for a spiral motion.

The spatial distribution of the masers in the N region presents an arc-like shape (see Fig. 2a), and Fig. 3N shows that the maser  $V_{\text{LSR}}$  increases linearly with the rotation radius  $R$ . The relatively large separation from the jet axis and radial extent suggests that the N stream is observed close to the plane of the sky. In this case, the maser  $V_{\text{LSR}}$  should mainly trace rotation. Then, the good linear correlation between  $V_{\text{LSR}}$  and  $R$  indicates that the masers co-rotate at the same angular velocity,  $\omega_{\text{N}} = 0.274 \pm 0.005 \text{ km s}^{-1} \text{ au}^{-1}$ . A simple interpretation is in terms of a magneto-centrifugally accelerated stream of gas emerging from a point of the disk. A disk in Keplerian rotation around an YSO of about  $5.6 M_{\odot}$  attains an angular velocity equal to  $\omega_{\text{N}}$  at  $R \approx 40 \text{ au}$ . Remarkably, the linear extrapolation to lower elevation and smaller radii of the arc traced by N stream intercepts the disk axis close to 40 au (Moscadelli *et al.* 2022, see Fig. 6a), as expected if the gas, launched from the disk, first streams approximately along a straight line.

In conclusion, the analysis of the kinematics of the water masers in IRAS 21078+5211 strongly indicates that a MHD disk wind is a natural frame to explain both the spiral motions traced by the masers close to the jet axis in the NE and SW regions and the gas

co-rotation along the N stream. Our interpretation is supported by (resistive-radiative-gravito-) MHD simulations of the formation of a massive star that lead to a magneto-centrifugally launched jet whose streamlines closely reproduce the maser patterns (see Fig. 2b). Presently, these results provide one of the best evidence for a MHD disk wind. Since water maser emission is widespread in YSOs, sensitive VLBI observations of water masers can be a valuable tool to investigate the physics of disk winds.

## References

- Blandford, R. D. & Payne, D. G. 1982, *MNRAS*, 199, 883–903.  
Moscadelli, L., Beuther, H., Ahmadi, A., *et al.* 2021 *A&A*, 647, A114.  
Moscadelli, L., Sánchez-Monge, Á., Goddi, *et al.* 2016, *A&A*, 585, A71.  
Moscadelli, L., Sanna, A., Beuther, H., *et al.* 2022, *Nature Astronomy*, 6, 1068–1076.  
Pudritz, R. E. & Norman, C. A. 1983, *ApJ*, 274, 677–697.  
Sanna, A., Moscadelli, L., Goddi, C., *et al.* 2018, *A&A*, 619, A107.